



Voltage-dependent gating in K channels: experimental results and quantitative models

Luigi Catacuzzeno¹ · Luigi Sforna¹ · Fabio Franciolini¹

Received: 1 August 2019 / Revised: 27 November 2019 / Accepted: 28 November 2019 / Published online: 20 December 2019
© Springer-Verlag GmbH Germany, part of Springer Nature 2019

Abstract

Voltage-dependent K channels open and close in response to voltage changes across the cell membrane. This voltage dependence was postulated to depend on the presence of charged particles moving through the membrane in response to voltage changes. Recording of gating currents originating from the movement of these particles fully confirmed this hypothesis, and gave substantial experimental clues useful for the detailed understanding of the process. In the absence of structural information, the voltage-dependent gating was initially investigated using discrete Markov models, an approach only capable of providing a kinetic and thermodynamic comprehension of the process. The elucidation of the crystal structure of the first voltage-dependent channel brought in a dramatic change of pace in the understanding of channel gating, and in modeling the underlying processes. It was now possible to construct quantitative models using molecular dynamics, where all the interactions of each individual atom with the surroundings were taken into account, and its motion predicted by Newton's laws. Unfortunately, this modeling is computationally very demanding, and in spite of the advances in simulation procedures and computer technology, it is still limited in its predictive ability. To overcome these limitations, several groups have developed more macroscopic voltage gating models. Their approaches understandably require a number of approximations, which must however be physically well justified. One of these models, based on the description of the voltage sensor as a Brownian particle, that we have recently developed, is able to simultaneously describe the behavior of a single voltage sensor and to predict the macroscopic gating current originating from a population of sensors. The basics of this model are here described, and a typical application using the Kv1.2/2.1 chimera channel structure is also presented.

Keywords Voltage-dependent gating · Voltage-gated potassium channels · Mathematical models · Gating currents

Introduction

Voltage-dependent ion channels are a class of transmembrane proteins capable of opening and closing in response to voltage changes across the membrane, and selectively conducting ions in and out of the cell. These features make them key players in

many biological processes in both excitable and non-excitable cells. Much effort has been put, over the last 40 years, in the comprehension of the mechanisms that make these proteins capable of sensing the voltage applied to the membrane, and to translate it into a conformational change leading to ionic fluxes. Although this paper will specifically address the voltage-dependent gating in K (Kv) channels, the first experiments that allowed to envisage the basic mechanisms of this process were done on native and cloned voltage-dependent Na (Nav) channels, which we present to give readers the essential background. In later paragraphs, we will instead focus on the experiments on Kv channels that allowed to understand the detailed mechanism governing their voltage dependence. Specifically, we will describe the functional experiments carried out in *Shaker* channels, where the voltage dependence has been widely studied, and because they are highly homologous in structure to the first channels for which a crystallographic structure was made available. In the second part of the review,

Notice For the benefit of a wider readership, several mathematical passages and demonstrations have been kept from the present review. Dr. Catacuzzeno will be happy to provide interested readers with all the demonstrations and information required.

- ✉ Luigi Catacuzzeno
luigi.catacuzzeno@unipg.it
- ✉ Fabio Franciolini
fabio.franciolini@unipg.it

¹ Department of Chemistry, Biology and Biotechnology, University of Perugia, Via Elce di Sotto 8, 06123 Perugia, Italy

we will present theoretical models capable to give a quantitative explanation of the voltage-dependent gating of Kv channels.

Early experiments and hypotheses of voltage-dependent gating

Voltage-dependent membrane permeability changes were seen for the first time about 70 years ago by Hodgkin and Huxley, when the concept of ion channels had not yet been elaborated. These permeability changes were postulated to depend on the presence of voltage sensors, in the form of charged or dipole particles that move through the membrane in response to voltage changes [35]. At negative voltages typical of resting neurons, the hypothetical positively charged particles would be positioned towards the intracellular side of the membrane and stabilized by the negative countercharges. Under these conditions, the membrane would not pass ions. Upon depolarization, the charged particles will move outward, and this very movement increases the membrane permeability to ions (Fig. 1a). Because these charged particles were seen to control the gating of ion fluxes, they were named gating particles.

Hodgkin and Huxley knew nothing, at the time, about the molecular nature of these gating particles. Nonetheless, they anticipated that their movement across the membrane would

originate a current—the gating current, for its association to the movement of gating charges—that precedes the rise of the ion currents. They further added, based on theoretical considerations and because they were unable to see them in a few trials they made at the Na equilibrium potential (to zero the Na current for better seeing them—TTX was not known then), that these currents had to be very small, hardly more than a few percent of the maximal Na current (a prediction that turned out to be essentially correct).

The next step was to record the gating currents as proof of the existence of the postulated gating particles. Several labs set out to record them, yet it was not until the early 1970s—more than twenty years after Hodgkin and Huxley had postulated their existence—that gating currents originating from Nav channels were finally recorded [5, 42, 70]. The reason for such a delay between their theoretical prediction and experimental observation comes from the difficulty of their measurement due to their small amplitude and fast and transient kinetics.

In the meantime, the gross architecture of voltage-dependent ion channels was beginning to be resolved. In 1984, Numa's lab published a milestone paper reporting the primary structure of Nav channel from *Electrophorus electricus* electroplax, as defined from its cDNA [60]. The channel protein was made of more than 1800 amino acid residues, and displayed the repetition of four similar

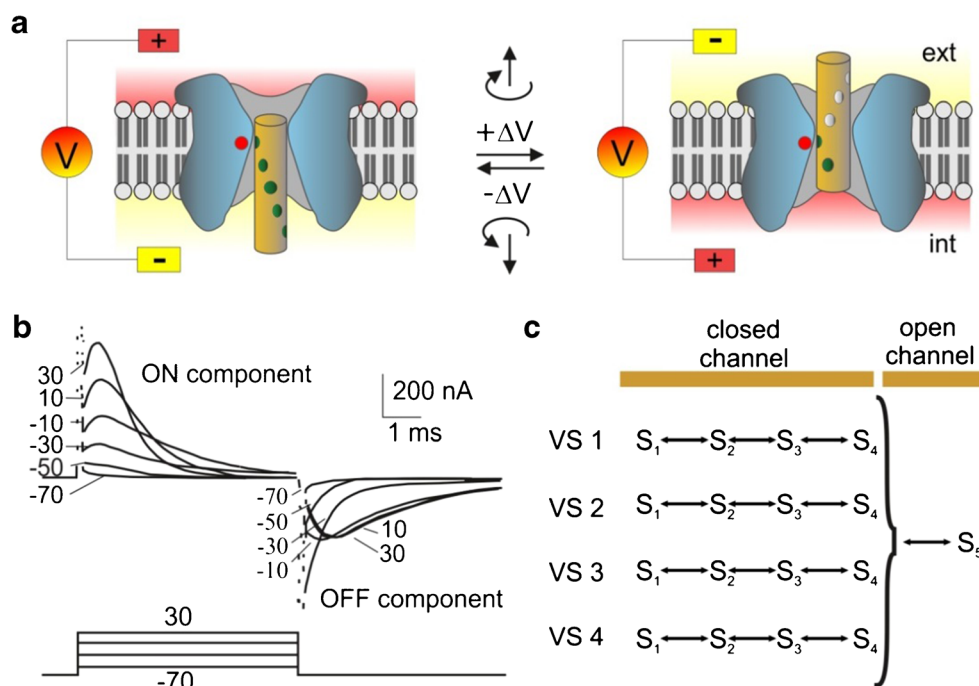


Fig. 1 **a** Drawings illustrating the sliding helix model of voltage-dependent gating of Kv channels. Upon depolarization, the electrostatic force keeping the voltage sensor—the sliding helix—fully inward (left sketch) is relieved, letting it slide outward along a helicoidal path (right sketch) such that positive charges (green) on the sliding helix establish in succession ion pairs with negative charges (red) present in the neighboring segments of the voltage sensor domain. Only one of the four sliding

helices/voltage sensors of Kv channels is shown in the figure. **b** Family of macroscopic gating currents evoked from *Shaker* channels subjected to membrane depolarizations from -70 to 30 mV (modified from Bezanilla, Perozo, and Stefani [10]). **c** Representative kinetic scheme containing the main features found by studying the properties of the macroscopic gating current in *Shaker* Kv channels

(homologous) domains (I–IV). Based on the hydropathy plot, each of the four domains was predicted to contain six transmembrane α -helical segments (S1–S6). Most interestingly, one of these segments, the S4, showed the striking feature of displaying 4 to 7 positive charges (usually arginine) systematically interposed by two non-charged, mostly hydrophobic residues. This immediately suggested the role of voltage sensor for S4 [16, 31, 32, 60].

An intense investigation began with the aim of verifying this notion. Many studies investigated the effects of neutralizing the charged residues on S4. Stühmer and Conti, in collaboration with Noda and Numa, carried out the widest functional analysis for the time by assessing the voltage sensitivity of several mutated Nav channels (with one or more positive charges removed, replaced by neutral or negative residues) expressed in *Xenopus* oocytes [69, 83]. They found that progressively reducing the overall net positive charge on S4 of repeat I resulted in a progressive and significant decrease of the apparent gating charge z_g (estimated from the limiting slope). Their results provided the first experimental evidence that S4 was the voltage sensor of the Nav channel, or at least part of it. Shortly afterwards the other two major voltage-dependent channels, Kv and Cav, were cloned and found to share the same overall architecture of the Nav channel: four domains (for Cav channels) or four independent protein subunits (for Kv channels), with each domain or subunit containing six transmembrane α -helical segments (S1–S6). Also, the S4 segments of both the Kv and Cav channels contained an excess of positive charges invariably interposed by two non-charged residues, and the replacement of these positive charges with non-charged residues decreased the channel's voltage sensitivity.

The accumulated structure–function data and the postulated overall architecture of the Nav channel based on its primary structure stimulated intense thinking about the gating mechanism of voltage-dependent channels. One of the central questions was how S4 containing 4 to 7 positively charged amino acids could be stabilized in a hydrophobic lipid environment and move outwards, translocating the gating charges across the membrane. In 1986, Catterall and separately Guy and Seetharamulu reached, with their respective *Sliding helix* and *Helical screw* models, similar mechanistic conclusions for the S4/voltage sensor motion (Fig. 1a; [15, 32]).¹ The positively charged amino acids on S4 were hypothesized to interact with negatively charged residues on neighboring helices, and form ion pairs which stabilize the S4 in a hydrophobic environment. At the resting (negative) cell membrane potential, the

positively charged residues pull S4 inwards by electrostatic forces. Upon release of these forces by membrane depolarization, S4s begin to move outwards in a spiral movement. This type of motion would allow for contacts to be made between helicoidally spaced charges on S4 segments and negatively charged residues on neighboring transmembrane domains (which mutation experiments later identified on S1 and S2 segments; [62, 86, 87]). Maximal displacement of S4 segments, from their most retracted position into the cell at very negative potentials to the most external position upon positive potentials, was estimated to be 13.5 Å normal to the membrane, and twisted by about 180°. This model of positively and negatively interacting charges resolved the thermodynamic problem posed by inserting the highly charged S4 segments in a hydrophobic transmembrane environment, and the sequential exchange of ion pair provided a low-energy pathway for gating charge movement.

Voltage-dependent gating in Kv channels

Macroscopic and microscopic gating currents originating from *Shaker* channels

Due to a lack of preparations expressing Kv channels at high density (as the *Electrophorus electricus* electroplax for Nav channels) and the delay in cloning their genes needed for their high expression in heterologous systems, the gating currents of Kv channels were first recorded only two decades after the Nav channels'. The voltage-dependent *Shaker* channel was the first to be cloned (from *Drosophila*; [61, 66]) and expressed on *Xenopus* oocytes, which allowed the first gating current recordings from Kv channels [9, 84]. It was found that both the ON and OFF gating currents showed quite a complex behavior, decaying monoexponentially for low depolarizing voltages, biexponentially at intermediate levels of depolarization, and additionally showing a plateau/rising phase followed by a monoexponential decay for high depolarizations (Fig. 1b; [10, 98]). This complex behavior, not predicted by a gating charge moving in only one step along its activation pathway, together with the sigmoidal time course of the ionic currents, suggested the presence of multiple transitions of the voltage sensor preceding the actual opening of the channel, each carrying a partial charge along the voltage drop.

In fact, multiple kinetic states were later found by interpreting experimental gating currents with discrete Markov models, that is, assuming very fast passages of the gating particles (voltage sensors) between energetically stable states [10, 58, 72, 90, 98]. The choice of using Markov modeling was based on the fact that it allowed to analyze and interpret experimental gating currents without having to know the structure of the ion channel and the voltage sensor that were both lacking at the time. The only parameters present in these

¹ Credit should be given to Clay Armstrong for proposing, few years before the elucidation of the primary structure of the Nav channel and deduced overall channel architecture, the sliding-ratchet model [4]. Here a voltage sensor with a row of positive charges would creep over a row of negative charges in an adjacent domain, thus acting like a zipper that forms and breaks ion pairs sequentially while it moves upward during channel activation.

models were the rate constants connecting the various states that were determined by fitting experimental data. Obviously, these models did not say much about the physics of the gating process, and more so about the underlying structure/function relationship, simply because they neither included structural data nor used physical laws. They however gave important clues in terms of the kinetic and thermodynamic comprehension of the process.

Markov modeling of *Shaker* gating currents was able to predict several important features of the gating mechanism.² First, it was found that the four voltage sensors of the channel would move mostly independently from one another, as shown by the kinetic scheme obtained by modeling the gating currents (Fig. 1c). Instead, there was a high level of cooperativity in the final step (or two last steps, according to Schwaiger et al. [71]) that brought the channel to open, allowing the four voltage sensors to concurrently make the final step, and assume the position which led to channel opening. Second, the movement of each voltage sensor was found to occur through multiple steps (four in the scheme shown, but the number varied slightly among different labs). Multiple steps for each voltage sensor, and different associated transition rates, were needed to explain the rising phase of the gating current seen at the beginning of the depolarizing step, as well as the multiexponential decay. In conclusion, Markov modeling did provide an overall understanding of the kinetics of the voltage sensors movement during channel activation, although there was scarce knowledge about the structures involved and their exact movement during the gating process. Notably, the types of kinetic schemes found for *Shaker* channel gating were well in accordance with the sliding helix hypothesis proposed several years before for Nav channels.

In addition to the slow ON and OFF components described above, the macroscopic gating current of *Shaker* channels, when high-speed recording was enabled, showed a very fast component, rising instantaneously and then decaying exponentially with a time constant of few tens of microseconds. This fast component was present both at the beginning of the depolarizing pulse and following the repolarization of the membrane potential [77] (in Fig. 1b, this component can be appreciated as a fast current peak at the beginning of the recording). This feature, which is not predicted by discrete Markov models, has been interpreted as a redistribution of S4 population within the energy wells occupied in the fully activated or fully deactivated state, following a sudden change in the membrane potential [77].

Investigation of the gating currents also provided reliable estimates of the number of charges that needed to move to

open a channel. This was assessed by measuring the total gating charge (as the time integral of the gating current) upon maximal activation, and dividing this amount by the total number of contributing channels. To avoid counting moving charges not involved in opening the channels of interest, experiments were carried out on *Xenopus* oocytes where channels were expressed at high density, which resulted in gating currents with negligible interference from other channels. Using this approach, consensus was reached for *Shaker* with a total of 12–14 eo moving to open one channel [1, 59, 72, 74].

The availability of essentially pure populations of channels, when expressed in *Xenopus* oocytes, gave also the opportunity to measure the fluctuation properties of the macroscopic currents, and provided critical information on the microscopic events. Using *Xenopus* oocyte macropatches expressing a large number of Nav channels, Conti and Stühmer [20] studied the fluctuations of the Nav gating currents to get clues on the type of movement of the voltage sensors within an individual Nav channel. They found that charge movement had the properties of a shot-like process with elementary charge transported of 2.3 eo. Notice however that the background noise of the patch clamp and biological preparation required heavy filtering that could be limiting for the fast Nav channels. When Bezanilla and coworkers studied the gating current fluctuation of the slower *Shaker* channels [76] using appropriate filter settings, they found a shot-like elementary charge of 2.4 eo, a result fully consistent with Conti and Stühmer's observations on Nav channels. These results suggested that the decaying part of the gating current could be explained by assuming the presence of a late step in the activation pathway carrying most of the gating charge [76].

The first five charged residues of the voltage sensor (the four arginines R1–R4 and lysine K5) are thought to contribute to the observed gating charge translocated in *Shaker* channels. Specifically, it was found that neutralization of either R1, R2, R3, or R4 led to a charge reduction of about 4 eo [1, 74] while neutralization of K5 gave discordant results, with a charge reduction of either 2 or 0 unitary charges [1, 74]. It was also established that the triplet periodicity (the charged residue followed by two non-charged ones) was essential for S4 to work effectively as a voltage sensor, and the hydrophobic residues interposed between the charged residues helped stabilize the resting state of the voltage sensor (by moving the half activation voltage of the Q-V curve towards more depolarized potentials).

The first 3D structures of Kv channels are provided

The picture radically changed over the first decade of the 2000s, when Roderick MacKinnon's group reported several x-ray crystal structures of Kv channels. The first high-resolution structure of a voltage sensor domain (VSD) was reported for KvAP, a K channel from the thermophilic

² Quite different kinetic models were however proposed in those years to describe the gating of *Shaker* channels [10, 58, 72, 90, 98], and the likely reason for the diverse modeling outcome is that different groups used different subsets of experimental data.

archaeobacteria *Aeropyrum pernix* [39]. In that structure, the voltage sensors were in a non-physiological conformation, displaced towards the intracellular side of the membrane and almost parallel to it. This observation, together with several functional data, oriented scientists towards the so-called paddle model of voltage-dependent gating, whereby the charge-bearing S4 forms a helix-turn-helix with the C-terminal half of S3 (S3b) that would translocate with a paddle-like movement the S4 gating charge on the opposite protein-lipid interface [75]. The situation radically changed few years later, when the structures of the Kv1.2 channel from rat [52], and a chimeric Kv1.2 channel containing the voltage sensor from Kv2.1 (Kv1.2/2.1 (paddle) chimera; [53]), were determined. These structures showed that the voltage sensor domain (S1–S4) was well conserved from prokaryotes to eukaryotes, and confirmed the tetrameric architecture of the channel, with the S5 and S6 segments of the four subunits making a central aqueous pore through which ions permeate, and the S1–S4 segments forming the four voltage sensor domains. These appeared to be located at the periphery of the central structure, loosely joined to the pore domain by four S4–S5 linkers, critical for coupling the voltage sensor movements to pore gating (Fig. 2c, d). As emphasized in the paragraphs below, the 3D crystal structure of the voltage sensor domain allowed to better understand the mechanism of voltage gating, and gave a clear explanation to many past and future functional experiments addressing the effects of amino acid mutations or chemical modifications of the channel structure.

S4 is surrounded by intracellular and extracellular aqueous vestibules separated by a very short water-inaccessible gating pore

Experiments from the 1990s, long before the generation of the channels' crystal structures, had already indicated that, within the VSD, S4 was mostly surrounded by wide vestibules that allowed entry of the aqueous solution. A first series of experiments, consisting in the substitution of different residues on S4 with the amino acid cysteine, were done to probe the ability of methanethiosulfonate (MTS; which is known to bind to cysteine) to modify the functional properties of the voltage-dependent gating, and gain clues on the accessibility to water of different portions of S4 in the varying conformational states. In other words, a modification of gating following the addition of MTS from the intracellular or the extracellular side would strongly suggest that the mutated position was accessible to the water solution via the internal or external vestibule.

MTS experiments indicated that at high negative potentials, corresponding to the deactivated conformation of the voltage sensor, R1 was accessible to water from the outside, R2 was accessible from neither side, and R3–K5 were accessible from the inside. Similar experiments, repeated at highly depolarized potentials that bring the voltage sensor in the fully activated

position, showed that now both R1 and R2 were accessible to the outside water, R3–K5 fully inaccessible, and R6 accessible from the inside [48]. The observation that large distal portions of S4 can be accessible to bulk water suggested that S4 can reach out on both sides into the relatively wide intracellular and extracellular vestibules. Only a very short portion of S4 (that varies with the functional state of the sensor) is inaccessible to water, indicating that it dwells in a physically narrow, high resistance region. Moreover, the substantial difference found at different applied potentials indicates that the segment moves for significant distances during the activation and deactivation process. Similar conclusions were reached with voltage-gated Na channels [95].

The presence of wide intracellular and extracellular vestibules separated by a short portion inaccessible to water was later confirmed by similar substitution experiments where, this time, the charged residues were replaced by histidine because of its ability to reversibly bind protons at physiological pH [80–82]. When histidine replaced R1, a proton current was observed at high hyperpolarization, which had the properties of a passive current through an ion channel [81]. When histidine replaced R4, a similar proton current was observed, provided that the membrane was highly depolarized. Considering that the charged residues R1 at hyperpolarized potentials or R4 at depolarized potentials occupy the central water-inaccessible region of VSD, the observed proton current could indicate that the short, high resistance region is likely formed by only one residue, which, when mutated to histidine, can connect the intracellular and extracellular environments and give rise to the proton current. The concept of a very narrow gating pore inaccessible to water and with high resistance was also suggested by other types of experiments that thoroughly investigated the region of VSD where virtually the full voltage drops [2, 6, 37].

As anticipated, the VSD crystal structure of Kv channels fully confirmed the picture derived from functional experiments. As shown in Fig. 2e, the S1–S4 segments of the VSD are indeed organized to form an hourglass-shaped structure with intracellular and extracellular aqueous vestibules separated by a thin hydrophobic barrier in which the key residue is represented by F233 (in Kv1.2/2.1 chimera). The Phe-based hydrophobic barrier, located about midway across the membrane and highly conserved in eukaryotic Kv channels, prevents water from either vestibules to pass to the other side, thus concentrating the whole electric field across a narrow central region of VSD. In this setting, the positively charged residues on S4 direct their lateral chains inside the aqueous vestibules, where they interact with water but also with highly conserved external (E183 and E226) and internal (E236, D259) negative clusters on the S1 and S2 segments. It is suggested that these negative residues, located on more stationary segments of VSD, would serve for anchoring (binding) in succession the S4 gating charges when membrane potential changes drive S4 up or down through the membrane.

The hydrophobic plug

Cysteine accessibility data together with mutagenesis results and molecular models suggested that the sliding pathway for S4 was essentially made by two water vestibules at the internal and external side of VSD, connected by a short and narrow portion inaccessible to water. The crystallographic structures of Kv and Nav channels later showed the presence at the beginning of the outer vestibule, next to the central narrow portion of their VSD, of a cluster of hydrophobic residues where water can hardly access. In the Kv1.2/2.1 chimera, besides F233, other nine residues (A319, V236, I241, C286, I320, I237, S240, F244, I287) appear to participate to the cluster and form this hydrophobic plug (Fig. 3a, orange residues). Due to their strategic position, each of them was systematically mutated to a large number of amino acids, and the kinetics and steady-state properties of the charge movement in response to membrane depolarization were analyzed for each mutant to understand the physico-chemical properties important for the gating process [47]. Notably, for some of the residues (I237, S240, F244, I287, and F290) the effects of the

mutation were highly correlated with either the size or the hydrophobicity of the substituting residue. Here we only draw attention to residue I287. It has been shown that the hydrophobicity at this position correlates strongly with a slow activation rate. It is noteworthy that at this very position, the Nav channel incorporates a much less hydrophobic threonine, and this is thought to critically contribute to the much higher speed of Nav channel activation than Kv channels' [46].

The N-terminal part of S4 assumes a 3–10 helix conformation

The crystal structures of Kv1.2/2.1 chimera channel disclosed another feature of potentially high relevance for the mechanistic understanding of the voltage sensor movement and its coupling to channel opening. The lower part of S4—below F233—was found to be structured as a 3–10 helix over a long stretch of amino acid residues (i.e., 7–11 or 2–4 helical turns) [53]. In this conformation, the amino acids are arranged in a right-handed helical structure. Each amino acid corresponds to a 120° turn in the helix (i.e., the helix has three residues per

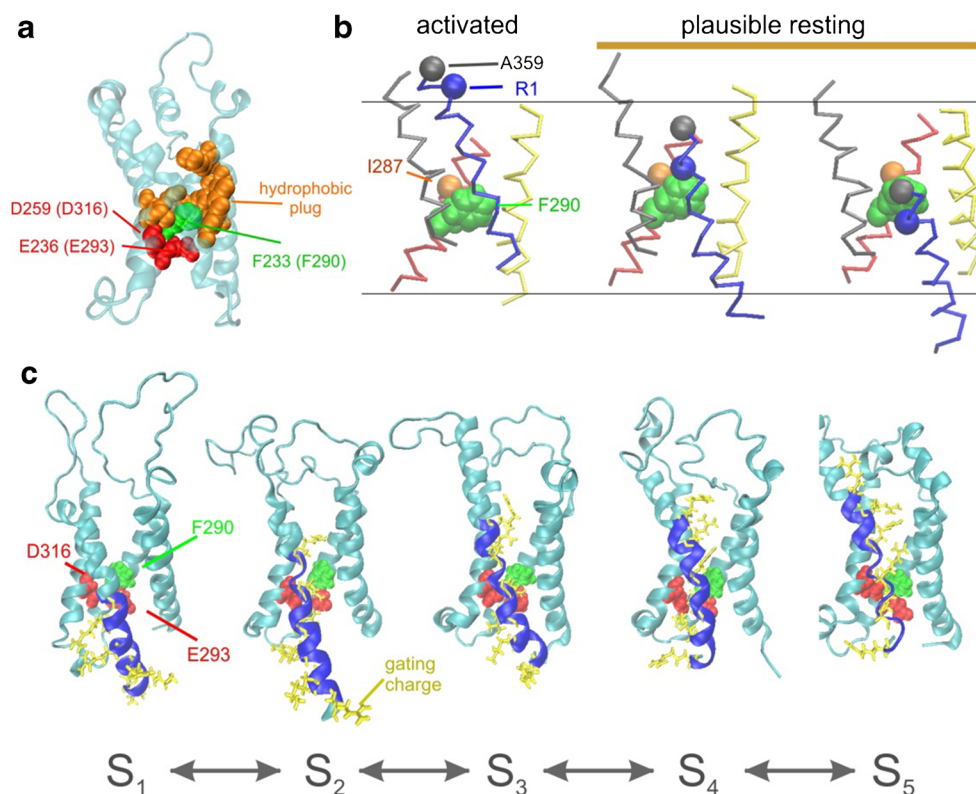


Fig. 3 **a** Representation of the voltage sensor domain of the Kv1.2/2.1 chimera, where the internal negative cluster and the hydrophobic plug have been explicitly shown with their van der Waals radius, and colored differently. **b** Schematic representation of the structure of the VSD in its activated conformation (left), and in its two possible resting conformations (center and right). The R1 gating charge and I287, A359, and F290 residues are explicitly represented. The three structures shown were taken from the *Shaker* channel model of Henrion et al.

(2012), states O, C3, and C4, respectively [34]. **c** Representation of the five sub-states of the VSD proposed by Henrion et al. for *Shaker* channel [34] showing the positive charges on S4 creeping over the GCTC, formed by the two negative charges D316 and E293, placed below F290 on adjacent domains, thus working like a zipper that cyclically forms and breaks chemical bonds while S4 moves upward during channel activation. The corresponding five-state kinetic scheme is illustrated below

turn), and a translation of about 2.0 Å along the helical axis, instead of 1.5 Å typical of the most common α (3.6–10) helix. Besides increasing the length of S4 by about 5 Å, this structure aligns vertically (as opposed to a helicoidal direction, as in the α helix) the gating charges on S4. If this mixed structure (α helix/3–10 helix) found in the open state of the channel (when S4 is maximally dislocated outwards) was fixed (that is, independent of the position of S4 along the gating pore), it would generate a mismatch for the gating charges to electrostatically interact sequentially with negative partners on neighboring segments while S4 moves inwards upon hyperpolarization. This would happen in any case, whether S4 rotated (as in the sliding helix model) or moved linearly—in one case, the mismatch would regard the gating charges on the 3–10 helix, in the other, the gating charges on the α helix.

Investigating the structure of the voltage sensor of the bacterial Nav channel NaChBac using molecular dynamics (MD) and experiments assessing the state-dependent interactions between the arginines on S4 and neighboring segments, Catterall's group also concluded that a portion of S4 is structured as 3–10 helix (from R1 to R4 in the resting states, and from R2 to R4 in the activated state [97]). A sequential dynamic transition between α helix and 3–10 helix occurring when S4 moves through the hydrophobic region of the gating pore has been suggested and partly validated by several simulations [23, 43, 73, 97]. Further investigation is needed to support this view.

Movements of S4 during voltage-dependent gating

The functional experiments reported above on MTS accessibility and proton transport induced by histidine mutations suggested that during the voltage-dependent gating, S4 moved so as to bring the R1–R4 gating charges across the high resistance region and give rise to the gating current. The amount and types of movements undergone by S4 remain an open issue. This point was first addressed using the fluorescence resonance energy transfer (FRET) technique which estimates the energy transfer between two light-sensitive molecules (chromophores, donor and acceptor) linked to specific parts of VSD. As the efficiency of this energy transfer is inversely proportional to the sixth power of the distance between donor and acceptor, FRET results extremely sensitive to small changes in distance, and useful to understand movements and distances at the space-scale of angstroms.

In a first series of experiments, donor and acceptor chromophores were placed at corresponding positions on different subunits of *Shaker*. When the chromophores were placed on S4, the change in efficiency in FRET during voltage-dependent gating was in accordance with a rotation of 180°, counterclockwise when observed from the extracellular side [17, 30]. In later experiments aimed at assessing the translatory movement of S4, one chromophore was attached to a

residue on the S3–S4 region, while the other was attached to a toxin bound on the channel pore, or alternatively on amphipathic ions residing on the plane of the membrane [18, 68]. Surprisingly, in both cases a very small translatory movement of S4 could be observed, amounting to less than 2 Å. This unexpected result, at odds with the sliding helix hypothesis, inspired a new model of channel gating, known as the transporter model, whereby intracellular and extracellular vestibules shaped as crevices would allow S4 to transfer the gating charges from one side to the other without making significant translatory movements, but by simply rotating. Subsequent FRET experiments performed using a higher number of residues found that the translatory movement amounted to about 10 Å, with a vertical component of about 5 Å [67], more consistent with the sliding helix model.

The crystal structures reported so far do not provide a conclusive answer in this regard. They position S4 of voltage-dependent K channels maximally projected outwards, with several gating charges exposed into the extracellular vestibule, indicating that the crystallized channel was captured in the activated, open state. To date, we have no crystal structure of voltage-dependent potassium channels in the closed state, making it difficult to understand the movement of S4 during the gating process. This has not prevented, however, from deriving models of the resting state based on both experimental and computational approaches [12, 22–25, 34, 38, 63, 93, 96, 97].

According to these models, channel closing involves S4 moving inwards while rotating counterclockwise when seen from the extracellular side [63, 92, 93]. Mean displacement of S4 along its main axis upon channel closing is about 14 Å, with a major rotation of about 180°, while the S1 and S2 segments retain essentially the positions they had in the open state. This would allow 3 positively charged arginines (R2 to R4) of S4 to pass from the extracellular to the intracellular vestibule of VSD, thus crossing virtually the entire membrane voltage drop, and giving rise to the experimentally recorded gating current. Note that in this proposed resting state, the R1 residue of S4 segments is placed above the highly conserved F233 emerging from the central portion of the S2 segment (cf. Fig. 3b, center structure).

Doubts on the position of R1 in the resting state

The resting state model described above, with the R1 placed extracellular to F290 (in *Shaker*), is in accordance with (in fact it was built using constraints based on) several experimental data from *Shaker* channels. First, the accessibility experiments showed that R1 remains accessible to extracellular MTS at very negative voltages [48]. Second, a mutation of E283 was shown to alter the proton current observed with the deactivated voltage sensor in channels carrying a second mutation in R1 [88]. Third, the double mutants R1C/I241C and R1C/I287C formed double cysteine bonds and froze the

channel in the resting state [12]. Since E283, I241, and I287 are all external to F290, these results indicated that in the resting state, R1 remains external to F290, occupying about the same position occupied by R4 in the open crystal structure.

However, other studies favored a different view. It was found that a tryptophan mutation at F290 (F290W) stabilized the open state in channels carrying a lysine in the fifth gating charge (i.e., in WT channels), likely by increasing its ability to interact with lysine. By contrast, the mutation stabilized the resting state when the first gating charge was mutated to lysine (R1K). These results suggest that, in the resting state, R1 occupies a position below F290, which in the open crystal structure is occupied by K5 [85]. In the same study, the authors emphasize the presence of two negative charges below F290, E293 in S2 and D316 in S3 that would form the GCTC capable of interacting in succession with R1 through K5 during gating [85]. Uncertainties thus appear still present with regard to the movement of S4 while closing, and the exact position of R1 in the resting state.

A more recent work has provided further evidence in support of the conclusion that in the resting state (i.e., at very negative voltages), R1 occupies the GCTC, i.e., lies below F290 [50]. To determine the position of R1 in the resting state, these authors used double mutations to histidine to take advantage of the property that two histidines, at appropriate distance (ca. 2.5–3.0 Å [3]),³ generate a binding site for Zn²⁺ ions, which would then link the two mutated residues together. Clearly, if one mutation is made on a residue located on a rather fixed segment of VSD, as S1–S3, and the other on S4, the generation of a Zn²⁺ bridge between the two mutated residues would significantly affect the voltage-dependent movement of S4. They started by mutating I287, which lies on S2 (ca. 7.8 Å above the GCTC), and R1. Measuring the effects of Zn²⁺ on channel gating (by assessing the kinetics of the ionic currents), they could estimate the relative position of the two mutated histidines, that is, the fraction of paired histidines bridged by Zn²⁺. They found that at a holding voltage of –80 mV, only a fraction of R1H was close enough to I287H, to form a binding site for extracellular Zn²⁺. This fraction further decreased—in other words, Zn²⁺-induced effects decreased—at more hyperpolarized holding voltages, suggesting that at voltages more negative than –80 mV, R1H had moved further inwards, likely overcoming F290 and binding to the GCTC.

They then wondered whether the inward movement of S4 at high hyperpolarizations would drag the initial portion of the outward loop linking S4 to S3 into the membrane. To clear this point, they paired mutation I287H with A359H,

located right at the beginning of the S4 outward loop, three residues above R1 (Fig. 3b), and again estimated their relative position from the effects of Zn²⁺ on the activation kinetics. Their results indicate that, at a holding voltage of –80 mV, corresponding to the resting state, S4 was in a position to bring a high fraction of A359H close to I287H and form binding sites for Zn²⁺, which would stabilize this conformation.

These observations, indicating a resting state with R1 below F290, in clear contrast with the results of Campos et al. and Tombola et al. [12, 89], could be reconciled with the latter studies by recalling that most of the results suggesting a position for R1 above F290 were obtained with R1 mutated to neutral residues. This occurrence introduced uncertainties since without a positive charge in R1, S4 could have not been able to reach its most inward position, typical of the resting state, because the charged R1 is exactly where the electrostatic force is exerted to fully push S4 inwards. On the other hand, also some experiments reported by Lin et al. [50], and more specifically those carried out with the mutation A359H, could be heavily biased. Mutation A359H that introduced a protonated histidine on the S4 segment could have in fact modified the overall charge on the voltage sensor, making equally uncertain the exact position of the S4 segment in the resting state.

Interactions between S4 and S5 segments

Several experiments carried out on *Shaker* suggest that S4 interacts with the pore domain in multiple places, and these interactions are important in channel gating. Tryptophan scanning mutagenesis showed that voltage-dependent gating can be affected by mutations of several residues placed on the pore domain [51]. Most of these residues that belong to the intracellular half of the S5 segment are able to interact with the hydrophobic residues V369, I372, and S376 of S4 [79]. Noteworthy, these residues were previously found to strongly affect the *Shaker* channel cooperativity when mutated to isoleucine, leucine, and threonine, respectively (ILT mutant [78]). Double mutant cysteine experiments have identified another region of interaction between S4 and S5, and found that when S4 is in the activated conformation, the region 354–362 (S3–S4 and proximal S4) is in close proximity to residues 416 (proximal S5) and 422 (the turret) [29].

Electromechanical coupling between S4 and the pore domain

Here we report some of the experiments that have partially clarified the mechanism linking the movement of the S4 segment to pore opening. Readers interested in the details of the electromechanical coupling are referred to specific reviews on the subject [11, 91].

Almost twenty years ago, Lu, Klem, and Ramu (2001) and Lu, Klem, and Ramu (2002) [54, 55] reported that it was

³ If two histidines participate in a zinc binding site, they must be within a few Å from each other given that the distance between the zinc and its coordinating atoms in catalytic zinc sites on histidine is ca. 2.1 Å. Considering the angles between zinc and the coordinating atoms according to coordination geometry of 70° to 100°, the effective distance between the coordinating atoms—i.e., the two histidines—is 2.5–3.0 Å.

possible to confer voltage-dependent gating to the intrinsically voltage-independent bacterial KCsA channel by adding to its pore module M1–M2, the VSD (S1–S4) module of *Shaker*, and associated linker S4–S5. They also found that in order to obtain a functional voltage-dependent channel, both the linker S4–S5 and the N-terminal S6 (S6T) had to come from the *Shaker* channel. Further studies explained why by showing that a region of S6T interacts directly with the S4–S5 linker of the same subunit and with the S4–S5 linker of an adjacent subunit. It was further shown that mutations disrupting these interactions shifted leftward the Q-V relationship but rightward the G-V relationship. This peculiar opposite effect on Q-V and G-V relationships suggested the uncoupling of the voltage sensor from the pore opening, within a framework where S4 is connected with the pore opening through the interaction between the S4–S5 linker and the S6T [7, 33, 45].

Additional information about the functional coupling between the voltage sensor and the pore was obtained by Kalstrup and Blunk who were able to simultaneously monitor the *Shaker* Q-V and G-V relationships and two different fluorescence signals associated with channel activation, using the double mutant XAnap/A359C [40, 41]. Anap is a non-natural intrinsically fluorescent amino acid that was substituted to various intracellular residues (*X*) supposedly implicated in the coupling process, and A359C, located at the beginning of S4 outward loop, was used to anchor, via cysteine, the second fluorescent compound to the extracellular end of S4. Collectively, these studies using fluorescent probes and biophysical approach indicated that the activation process develops in three successive steps: (i) an initial movement of S4 that drags only the N-terminal portion of the S4–S5 linker. These movements, which are observed experimentally at mild negative potentials, occur independently in the four subunits of the channel; (ii) a further shift of S4 that now pulls the whole S4–S5 linker occurs with intermediate depolarizations; (iii) the full translocation of S4 and S4–S5 linker that results in the opening of the pore. This last step requires high voltages and the concomitant involvement of the four subunits.

More quantitative information on the movement of the S4–S5 linker during channel opening was obtained by inserting acceptor and donor chromophores in various residues of the linker, and probing their movement with the FRET technique. It was found that, during the closing of the channel, the S4–S5 linker comes closer to the pore (by 3.4 Å) by moving outward the C-terminal part, while rotating around its long axis by 17° [40].

Notably, the electromechanical coupling properties observed in *Shaker* channels do not appear to be generally shared among voltage-dependent K channels. In KCNQ1 channels, it has been observed that several mutations in the S4–S5 linker and S6T region result in a tendency of the channel to remain constitutively open [56, 91], an effect going in the opposite direction as compared with that observed in *Shaker* channels.

Based on these results, it has been proposed that in KCNQ1 channels, the pore domain is more stable in the open than in the closed conformation, and uncoupling results in increased tendency of the channel to open [91].

Investigating the dynamics of the voltage sensor

The availability of the 3D crystal structure of the VSD from several Kv channels has been determinant for the quantitative understanding of the physical principles that make these proteins capable of sensing the membrane potential. The challenge was to thoroughly understand the structure/function relationship of voltage-dependent gating by applying modeling approaches that, unlike the discrete Markov models, use the now available structural information, and apply known physical laws to predict the movement of the voltage sensor, following electric field changes across the membrane. Two main types of approaches have mostly been used: the all-atom molecular dynamics and macroscopic approximation.

Molecular dynamics

Proteins are dynamic structures that vibrate internally over many timescales, and switch among several conformational states, which are often associated to specific biological functions. All these movements may in principle be predicted by using an MD approach. MD simulation is an established method for modeling these molecular movements of proteins, including ion channels, starting from known 3D crystal structures at high resolution (< 4 Å). However, crystal structures provide static images of proteins, and only in specific conformational states. Therefore, if we want to know how proteins behave and switch among different stable states, MD simulations appear in principle to be the first choice as, strictly speaking, they are the only ones capable of providing a reliable picture of proteins' motion at spatial and temporal domains that are not experimentally accessible.

MD simulations can explore the motion of ion channels, or functionally important portions of them, by solving the equations of motion of classical physics for all the atoms of the protein, from their initial positions derived from the crystal structure. At each step, the force acting on each atom has to be assessed by considering both strong (covalent) and weak (van der Waals and electrostatic) interactions with all the atoms in the surroundings, and the movement of the atoms is predicted in accordance with the net force acting on them. In spite of the inherent difficulties encountered by using this method, mainly related to the computational efficiency (see below), several useful results have been obtained by applying MD to voltage-dependent gating.

MD confirms the presence of intermediate states of the voltage sensor

Starting from the activated state of the Kv1.2 channel (called state alpha) and applying a strong hyperpolarization, Delemotte et al. [26] were able to follow the initial movement of S4 towards the intracellular side of the membrane. Interestingly, they found two relatively stable intermediate positions of the voltage sensor (called beta and gamma states), corresponding to the passage of R4 and R3 through the gating pore and the arrival of R3 and R2 in the GCTC. By applying a motion restraint, able to accelerate the gating process, these authors also found two additional states for S4, called delta and epsilon. The total gating charge estimated for the passage of the channel from alpha state to state epsilon amounted to about 12.8 eo, a value quite close to the experimental 13.5 eo found in *Shaker*. Notably, in the state epsilon, R1 appears positioned extracellular to the phenylalanine, although the charged group seems to be oriented towards E2 of the GCTC. Thus, this MD study seems to confirm the presence of intermediate stable states of S4, in accordance with what was previously proposed by a number of experimental studies and by Markov models.

Using MD and making use of the Rosetta method, and restrictions based on experimental data about the reciprocal position of S3 and S4, Henrion et al. [34] were able to find 5 stable conformations of VSD in the *Shaker* channel, where the positive charges from R1 to K5 occupy in succession a highly stable position below F290 and above the two stabilizing intracellular counter charges of the GCTC (Fig. 3c). These results, besides being coherent with Markov models suggestions, also confirmed the sliding helix hypothesis. According to this model, during the closing of the channel, S4 translates inward while rotating counterclockwise. This will allow 3 or 4 positively charged arginines of S4 to pass from the extracellular to the intracellular vestibule of VSD, thus giving rise to the experimentally observed gating current. During the voltage sensor movement, gating charges follow a common helical pathway, in order to be stabilized by the negative charges on neighboring segments of VSD.

Simulation of a complete gating transition

Using a supercomputer customized for MD studies (Anton), Shaw and coworkers have simulated the complete deactivating and activating trajectories of the voltage sensor of Kv1.2/2.1 chimera in response to very high membrane potential differences (to push S4 fast enough to complete its movement in about 1 ms) [38]. The simulation shows that in response to this very strong hyperpolarization, there is a fast closure of the pore promoted by the so-called dewetting (water tends to leave the intracellular vestibule, thus allowing the hydrophobic interaction among the amino-acidic residues), due

to a minimal movement of the four voltage sensors. Then, the four S4 segments move independently towards the intracellular side, making a translation of about 15 Å accompanied by a counterclockwise rotatory movement. Also in this case the computed total gating charge amounts to 13.3 eo, a value quite close to that experimentally observed for *Shaker* channel. By imposing a strong depolarization to the previously reached deactivated state, the authors were also able to obtain a reactivation of the four voltage sensors. Undoubtedly, this simulation represents a strong quantitative evidence for the sliding helix hypothesis, with an evident translatory and rotatory movement of S4 bringing several gating charges across the high resistance region.

Limitations of the MD approach

Even if potentially very useful, atomic level simulations are computationally extremely demanding since one needs to describe very fast events that happen at the atomic vibrational timescale of $\sim 10^{-15}$ s, which means to discretize the simulation at the level of femtoseconds. When this heavy discretization is coupled with the high number of atoms that need be considered for a reliable analysis and the computer time required to carry out one single calculation step, the total length of simulations that can presently be obtained on most lab computers is orders of magnitude lower than the timespan of most experimentally observed and functionally relevant processes.

Improvements in MD algorithms and computers performance are however rapidly expanding the studied timescale. From the 9.2 ps of the first all-atom MD simulation of a small protein in vacuum (bovine pancreatic trypsin inhibitor), carried out about forty years ago [57], we witness present simulation times rapidly approaching the timespan of biophysically relevant processes. However, apart from isolated exceptions, protein dynamics close to millisecond timescales (the functionally and experimentally relevant time domains) is currently inaccessible to conventional dynamics simulation in most laboratories.

Another shortcoming with MD regards verification and validation of its modeling output. There has been substantial agreement among scientists over past decades that computer models, in order to be scientifically sound, need to be validated, that is, checking that their output essentially agrees with the experimental results derived from the system studied. For channel voltage gating, the main experimental results presently available are the macroscopic gating current, measured in response to voltage changes. To be validated, a model of voltage gating thus requires to be able to simulate this quantity. All-atom MD is currently capable to output at most a microscopic gating current, that is, a gating current produced by the movement of only one sensor, or at best, one channel in response to a voltage step. This essentially means that although

useful to give some clues on the mechanism of channel gating, all-atom MD can hardly provide a validated model of voltage gating.

Alternative approaches are needed

To overcome these limitations, several alternative approaches have been developed, which share the aim of simplifying the system studied by applying reasonable approximations, yet fully retaining the potential to give basic information on the dynamics of voltage gating. Additionally, these alternative approaches have the relevant feature of providing a validated model, capable of outputting the Q-V relationship or the macroscopic gating currents.

A first attempt at building a macroscopic model of voltage-dependent gating was made by Peyser and Nonner in 2012 [64, 65]. In their model, S4 is represented by point charges embedded in a homogeneous dielectric that represents the rest of the protein, and incorporated into a simulation cell composed of a membrane dielectric, bath dielectrics and encapsulating electrodes. Fixed negative charges on S1–S3 were also included in the model, and allowed to interact with the gating charges. Therefore, instead of treating individually the atoms composing the protein voltage sensor, in this mesoscale model, the essential domains are considered as rigid bodies having the electrostatic features needed to promote voltage gating.

Using this geometrical setup, these authors assessed the energetic stability of the various possible configurations of the voltage sensor using statistical mechanics, and the relation between membrane potential and displaced gating charge could be constructed and compared with experiments. Peyser and Nonner observed a very robust behavior of the model with an electrostatic stability of S4 conferred by the surrounding countercharges, and with a quite high predictive ability when compared with experimental data. By comparing the behavior of models having S4 in the α and 3–10 helix configurations, the model suggests that only the α configuration is able to predict a Q-V relationship with features similar to those experimentally observed. Unfortunately, this model was only developed to assess the equilibrium position and stability of S4, and thus does not predict dynamic features of the voltage gating, such as the macroscopic gating currents.

A second model of this kind applied coarse-grained MD on the available Kv1.2 open crystal structure and intermediate/resting model structures, in order to assess the energetic profile encountered by the voltage sensor during its activation. This energetic profile was then used in a Langevin dynamics to predict the macroscopic gating current obtained in response to a depolarizing step [27, 28, 44]. Notably, this multi-scale modeling approach was able to predict the main kinetic features of the gating current, such as the fast gating current

component and the rising phase present at relatively depolarized potentials.

A recent macroscopic model of voltage-dependent gating was proposed by Bezanilla and coworkers [36]. In this model, where they use a Poisson-Nernst-Planck formalism, the gating charges are attached to S4 through hook springs, and allowed to move through the gating pore and intracellular and extracellular vestibules in response to an applied potential. This charges movement in turn transfers, through the attached springs, a force to S4 that promotes its sliding. Namely, arginines are treated as particles whose diffusion inside the voltage sensor domain in response to an electrical and chemical gradient is described by the Nernst-Planck equation, and the electrostatic potential profile is self-consistently computed using the Poisson equation, considering all the charges present in the system. By adjusting the free parameters of the model (essentially represented by the spring constants and mobility of the particles), the authors were able to reproduce the main features of the gating currents experimentally observed for *Shaker* channels. A pitfall of the model could be represented by the complete lack of countercharges that are instead known to be very important in real voltage-dependent gating.

We have recently developed a model of voltage gating that goes along this line, being based on the formalism of Brownian dynamics [13]. In Brownian dynamics, the movement of the particle of interest—the voltage sensor in our case—is assessed without considering individually the surrounding particles at atomic detail. Because they are so many and their collisions are so frequent, in the time scale of interest—the timescale of the gating process, i.e., milliseconds—their effects may be approximated by a random variable of the force acting on the particle of interest. In Brownian dynamics the Newton's law of motion of MD is thus replaced by the Langevin equation of motion which allows to describe the movement of a particle without having to consider explicitly all the atoms present in the surrounding. Below, we will illustrate the basics of the Brownian model developed, and an application of this approach to the voltage-dependent movement of S4 in a VSD having geometric and electrostatic properties congruent with the Kv1.2/2.1 chimera crystallographic structure.

Brownian motion as a reduced model of voltage-dependent gating

The theory of Brownian motion is possibly the simplest approximate way to treat the dynamics of non-equilibrium systems in a physically consistent way. It was developed to explain the original observation of the biologist Robert Brown on the movement of pollen grains and dust particles in water that showed frequent and unpredictable changes in the velocity and direction of motion. This theory can be applied when a relatively large particle (the Brownian particle, with typical

dimensions in the nanometer to micrometer range) moves in a fluid of much smaller particles, for which the knowledge of the exact dynamics is not required. Although Brownian particles are themselves made of much smaller atoms, their movement can be approximated to the motion of a rigid body, and its dynamics can be described by the movement of its center of mass. Due to the very different dimensions, the thermal motion of the surrounding atoms making up the fluid will be much faster than the motion of the Brownian particle. Typical relaxation times—the time a particle takes to move over a distance equal to its own radius—of the atoms of the fluid are in the 10^{-12} s range (τ_S), compared with the Brownian particle's ranging around 10^{-3} s (τ_B). Under these conditions, the motion of the Brownian particle over the longer time scale τ_B may be described by tracking the trajectory of its center of mass, without having to consider in detail the motion of the surrounding atoms (see below), but concentrating on the particle of interest.⁴

In the case of the voltage sensor domain, on which we are going to apply this treatment, the Brownian particle is represented by the charged S4 segment whose motion generates the gating current and promotes channel opening. The surrounding atoms are instead represented by water molecules, ions, lipids, and other atoms of the VSD, with which S4 interacts while moving. Although we are not directly interested in their dynamics, they will be indirectly considered in order to realistically describe the dynamics of the Brownian particle.

Dynamics of the Brownian motion

We will first recall the reasoning that brought Langevin to propose a simplified description of the dynamics of the Brownian particle [49]. For simplicity, we will consider motion in only one dimension. He started by postulating that the motion of the Brownian particle, like the motion of any other particle, needs to be in accordance with Newton's second law, stating that the acceleration of a particle is proportional to the force acting on it: $m \frac{dv(t)}{dt} = F(t)$, where m is the mass of the particle, $v(t)$ its time-dependent velocity, and $F(t)$ the force acting on the particle. In the hypothetical case of a particle moving in an empty space with no surrounding atoms, $F(t)$ could only be an “external” force, that is, a force originating from a gravitational, electrostatic, or magnetic field present in the region where the particle is placed. In the case of S4, the external force is most likely dominated by the electrical force acting on the gating charges moving in a varying electric potential (V): $F_{ex}(t) = -\sum_i q_i \left(\frac{dV(x)}{dx} \right)_i$, where q_i are the gating

charges, and the sum goes over all the gating charges on the voltage sensor.⁵ In fact, the Brownian particle does not move in an empty space, but in a fluid made of much smaller particles that constantly collide with it, contributing in this way to the net force acting on the Brownian particle, and as a consequence to changing its velocity and direction of motion.

Langevin proposed to divide the contribution of the surrounding atoms to the cumulative force acting on the Brownian particle into two main components. A frictional force that opposes the movement of the Brownian particle, originating from the viscous medium in which the particle is immersed, and a collision force exerted on the Brownian particle by surrounding atoms and molecules. The frictional force may reasonably be expressed by a term proportional to the velocity of the particle, where γ is the frictional coefficient that describes the frictional effects that water and surrounding protein structures have on the motion of S4. The second parameter, the collision force, accounts for the passage of energy from the surrounding to the Brownian particle, as a result of the collisions. This term yields that at equilibrium a certain amount of energy will always be associated with the Brownian particle. Because of the fast movement ($\tau_S \sim 10^{-12}$ s) and high number of surrounding atoms, the Brownian particle will receive millions of collisions during the millisecond time scale of its gating motion, and in each small timestep, the particle will change, in an essentially random way, the applied force by an amount $F_\epsilon(t)$. In contrast to the external and frictional forces, $F_\epsilon(t)$ may thus be considered a random variable that can be defined by its probability density function that Langevin proposed to be Gaussian in shape, with zero mean ($\langle F_\epsilon(t) \rangle = 0$).⁶

Langevin further proposed that the second moment of the distribution has a shape $\langle F_\epsilon(t) F_\epsilon(t') \rangle = B \delta(t - t')$ determined by the Dirac delta function $\delta(t - t')$ ⁷ which ensures that the second moment is nonzero only when $t = t'$, that is, this random force is uncorrelated in time (no relation exists between two forces at two different times). Although this is not the case on the time scale characterizing the motion of

⁵ Notice that each gating charge will experience a different force, given by the electric potential gradient present at its own location. Thus in order to assess the “external force” acting on the voltage sensor, the electric potential profile $V(x)$ must be assessed. This may be done in a physical consistent way using for example Coulomb's law for a system composed of particles at discrete locations, or Poisson's equation for systems with a more diffused charge density, by including the contribution of all the charges present in the system and of the potential difference applied.

⁶ Justified by the fact that we have already considered the average force contributed by the surrounding by including the frictional term.

⁷ The Dirac δ function is a generalized function or distribution introduced by the physicist Paul Dirac. It is used to model the density of an idealized point mass or point charge as a function equal to zero everywhere except for zero, and whose integral over the entire real line is equal to one.

⁴ This is a major point when compared with MD, where the dynamics of all the atoms in the system has to be assessed.

the surrounding atoms,⁸ this assumption becomes acceptable on the time scale typical of the Brownian particle dynamics, since even within a time interval that can be considered small for this time scale (let us say one hundredth of τ_B), there will still be hundreds of thousands of collisions that memory can be considered lost. B is a measure of the strength of the fluctuating force, and it can be shown to be equal to $2k_B T \gamma$. In conclusion, for a Brownian particle moving in presence of an external force, we arrive at the following Langevin equation:

$$m \frac{dv(t)}{dt} = F_{ex}(t) - \gamma v(t) + F_\varepsilon(t) \quad (1)$$

where $F_\varepsilon(t)$ has a Gaussian distribution, with $\langle F_\varepsilon(t) \rangle = 0$ and $\langle F_\varepsilon(t) F_\varepsilon(t') \rangle = 2k_B T \gamma \delta(t - t')$.

Now we will show that at the nanometer scale of our Brownian particle—S4/voltage sensor—the inertial term $m \frac{dv(t)}{dt}$ can be fully neglected. In evaluating the relative contribution of the inertial ($F_{inertial} = m \frac{dv(t)}{dt}$) and viscous ($F_\gamma = -\gamma v(t)$) terms in the above equation, let us first consider an object of typical size a and density ρ , moving with velocity v in a fluid. The inertial term may be approximated as $F_{inertial} \approx \rho a^3 v \frac{v}{a} \approx \rho a^2 v^2$ while the dissipative (frictional) force, from Stoke's law, by $F_\gamma \approx v a \mu$, where μ is the viscosity of water (10^{-3} Pas). The relative contribution of the two forces is captured by the Reynold's number $Re = \frac{F_{inertial}}{F_\gamma} \approx \rho a v / \mu$. Our daily experience of objects motion in fluids relates to the realm of large Reynolds numbers. For example for a fish swimming in water, we would have $\rho \approx 10^3 \text{ Kg/m}^3$, $a \approx 1 \text{ m}$, $v \approx 1 \text{ m/s}$ giving a Reynold's number $Re \approx 10^6 \gg 1$ (taking density and viscosity of water). This means that in the visible world, the inertia term is very important and thus governs the dynamics of objects. The situation is quite different at the nanometer scale. In the case of our S4 segment, we would have $a \approx 10^{-9}$, $v \approx \frac{10^{-9} \text{ m}}{10^{-3} \text{ s}} \approx \frac{10^{-6} \text{ m}}{\text{s}}$ giving $Re \approx 10^{-9} \ll 1$.

Thus, as anticipated, at the nanometer scale of our system, the inertial term can be neglected, and the dynamics will essentially be governed by the dissipative term. Consequently, the Langevin equation under these highly damping conditions becomes $\frac{dx}{dt} = \frac{1}{\gamma} F_{ex}(t) + \frac{1}{\gamma} F_\varepsilon(t)$, and for the properties of the stochastic term illustrated above, it can be rewritten in the usual form for stochastic differential equations

$$dx = \frac{1}{\gamma} F_{ex}(t) dt + \sqrt{\frac{2k_B T dt}{\gamma}} \Phi(t) \quad (2)$$

⁸ Since a certain force at a certain time will have consequences on the force acting on the particle at a short interval later.

where $\Phi(t)$ is a normally distributed random number having zero mean and unitary standard deviation. Using this equation, the trajectory of a single Brownian particle may be followed for relatively long times using a commercially available personal computer, by simply reiterating the discretized form of the equation.⁹

Treating the S4 voltage sensor as a Brownian particle

The Brownian dynamics approach described above may easily be applied to describe the dynamics of S4 during gating. To this end, we first need to define the structural and electrostatic features of the model by referring to the available crystallographic structures of the VSD. In the illustrative application of the Brownian model to channel gating, here we refer to the Kv1.2/2.1 chimera channel. In the model, the voltage sensor domain is approximated by a simple geometrical structure consisting of a short water-inaccessible cylindrical gating pore flanked by an internal and an external water accessible vestibules opening with a half angle of 15° into two hemispherical subdomains of bath solution. As shown in Fig. 4a, this geometric shape adapts quite well to the structure. The vestibules (and baths) are filled with a solution containing 140 mM of positively and negatively charged monovalent ions that can freely move in the vestibules,¹⁰ but not in the gating pore. The water-inaccessible gating pore is placed at the level of F233, proposed to separate the internal and external vestibules of the voltage sensor domain. In the model, the moving S4 segment is represented by a charge profile (Z_{S4} , expressed in eo units, Fig. 4b) consisting of six positive charges, whose position was taken from the crystal structure. Note that in our model the R1 position that is uncharged in the chimera channel is assumed to carry a charge as observed in *Shaker* channels. In the simulation, the segment is allowed to move through the gating pore and vestibules up to a maximal displacement of 3.3 nm, enough to let the assumed five charged residues, R1 to K5, pass through (or reach, in the case of K5) the GCTC. The model also considers the charge profile of the fixed charges residing in the regions of the voltage sensor domain adjacent to S4 (Z_F , Fig. 4b). This charge profile was assessed from the crystal structure by measuring the position of all positive and negative charges in the S1–S3 segments of the VSD (indicated as yellow and red residues in Fig. 4a). The electrical potential profile $V(x)$ was assessed from the net charge density profile $\rho(x)$ using the Poisson equation [14] $\frac{\partial^2 V(x)}{\partial x^2} = \frac{\rho(x)}{\varepsilon \varepsilon_0}$ where $\varepsilon \varepsilon_0 = 8.85 \cdot 10^{-12} \text{ F m}^{-1}$ is the vacuum permittivity, and ε is the

⁹ For example, if X represents the position of the particle at time t , the position of the same particle after a short time Δt can be assessed. Each iteration is reassessed by considering the newly obtained position of the Brownian particle and the electrical force acting on it, and a new normally distributed random number is obtained from standard generator algorithms.

¹⁰ Ions were subjected to electro-diffusion governed by a flux conservative equation.

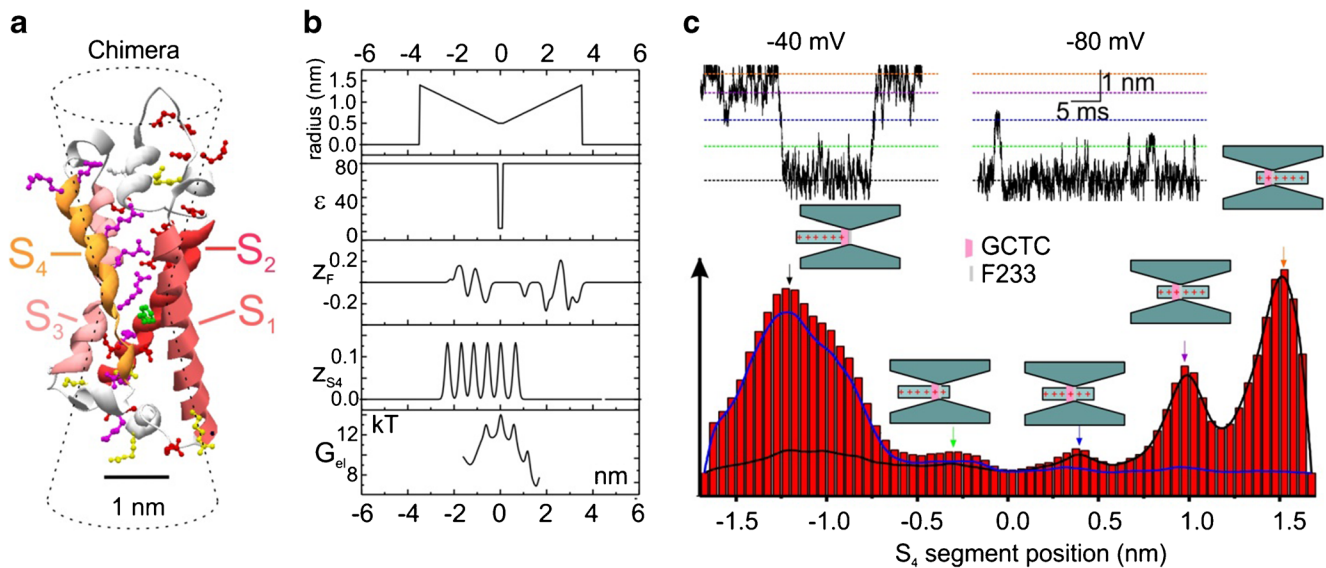


Fig. 4 **a** Representation of one VSD from the Kv1.2/2.1 chimera (structure 2R9R). Gating charges on the S₄ segment are magenta; negative and positive residues in the other segments of the VSD are red and yellow, respectively; residue F233 is green. The hourglass-shaped drawing superimposed to the VSD structure represents the geometry used in our model to delimit the gating pore and vestibules. The superposition shows that 15° as half angle aperture used in the model approximates quite well the shape of the vestibules. **b** Profiles of the gating pore radius, the relative dielectric constant (ϵ), the fixed charge density in the S₁–S₃ region of the VSD (Z_F), the charge density on the S₄ segment (Z_{S4}), and the electrostatic energy profile, G_{el} , assessed for all possible positions of the S₄ segment. In our model, the pore radius and Z_F are input parameters directly provided by the crystallographic structure (panel **a**); ϵ , the relative

relative dielectric constant, set at 80 in the ionic solutions and water accessible vestibules, and 4.0 within the water-inaccessible gating pore.

Simulation of the S₄ voltage sensor with the Brownian model

Figure 4 **c** (upper traces) shows representative simulations of the dynamics of one S₄ obtained by solving the stochastic differential Langevin equation at two different (indicated) membrane voltages. Several features are noteworthy from these stochastic simulations. First, S₄ tends to assume an intracellular position at very negative voltages (i.e., -80 mV), while it occupies more outward positions when the applied voltage becomes more depolarized, in accordance with a voltage-dependent gating. Second, while moving along its activation pathway, S₄, besides greatly preferring the most activated and deactivated positions, tends to dwell for significant times at three additional intermediate positions. This is clearly evident in the frequency histograms of the time spent by S₄ in the various positions assessed from a 100-ms simulation (Fig. 4**c**), where five preferential locations corresponding to the five peaks of the frequency amplitude histograms (indicated by arrows) are observed. In Fig. 4**c**, the positions that S₄ assumes

dielectric constant, is also an input parameter set to 80 in water accessible regions and 4—a value usually assigned to protein interiors—in the water-inaccessible gating pore. G_{el} represents instead an output of the model. We verified that the sharp change in ϵ at the vestibule/gating pore interface was not responsible for any of the qualitative aspects presented by the output of the model. **c** Top: Time courses of the position of the S₄ segment, obtained from stochastic simulations at two different voltages. Bottom: Amplitude histogram obtained by merging the two simulated traces at -40 and -80 mV, shown above. The five drawings associated to the five peaks of the amplitude histogram illustrate the positions within the VSD where the S₄ segment spends most of its time. The blue and black lines represent the amplitude histograms obtained by considering separately the data at -40 and -80 mV, respectively

in the gating pore in correspondence with each peak of the histogram are also sketched. These sketches show that the 5 states predicted by the model correspond to the positions of S₄ that allow different gating charges to interact with and rest in the GCTC. In other words, along its activation pathway from the resting to the activated state, S₄ mostly resides in one of the 5 sequential sub-states, which it occupies in turn by exchanging the gating charges position, in accordance with the classical sliding helix and the newly proposed GCTC hypothesis.

To further explore the origin of the 5 sub-states characterizing S₄, we assessed the electrostatic energy associated with the segment for all its possible positions (lower plot in Fig. 4**b**). Five energy wells are evident that will give rise to 5 stable positions of the voltage sensor. Looking at this energy landscape, with energy wells separated by energy barriers, it may be tempting to suggest that the voltage sensor may well be described by a Markov model with five distinct sub-states linearly connected. It needs to be mentioned, however, that theoretical calculations made using Kramer's diffusion theory suggest that well-defined Markovian states have to be separated by barriers at least 4–5 $k_B T$ high [21]. If the barriers are lower, then the movement of the particle may deviate from a fast hopping between sub-states. Notably, in our model

several energy barriers are of $\sim 2\text{--}4 k_B T$, and they become even lower at more depolarized or hyperpolarized voltages (not shown). This suggests that channel gating may have properties not predicted by Markov models.

From the dynamics of a single Brownian particle to macroscopic gating currents

As we have seen, the description of S4 as a Brownian particle allows to follow its trajectory for times long enough to fully cover the voltage-dependent activation process. These features allowed our Brownian dynamics model to confirm the conclusions suggested by the experiments and indicated by MD about the presence of multiple sub-states representing different S4 positions within the VSD. Yet, the ability of our model to describe the dynamics of a single gating particle over the full gating process is not sufficient for its validation, since validation requires comparing the model output with experimental data, which at the present time essentially consist of macroscopic gating currents originating from thousands of identical voltage sensors moving under the influence of voltage changes.¹¹

The description of S4 as a Brownian particle has however the provision to predict the macroscopic gating current. The dynamics of the Brownian voltage sensor, whose single particle position is described by the stochastic differential Eq. (2), may also be described in terms of the time evolution of the probability density function for the position of the particle, using the following Fokker-Planck equation [19]:

$$\frac{df(x, t)}{dt} = -\frac{1}{\gamma} \frac{\partial(F_{ex}(t)f(x, t))}{\partial x} + \frac{k_B T}{\gamma} \frac{\partial^2 f(x, t)}{\partial x^2} \quad (3)$$

Here $f(x, t)$ represents the probability density function of finding the Brownian particle at position x , at time t . The first term in the right-hand side represents, in analogy to the stochastic differential equation for the single particle dynamics, a drift term responsible for the movement of the particles in response to an external force, $F_{ex}(t)$, while the second term is the diffusion term, related to the thermal random agitation of the particles. Notably, the information above may readily be used to assess the macroscopic gating current produced by a population of voltage sensors behaving in accordance with Brownian particles, which in our model of the voltage sensor can be obtained as the time changes in the net ionic charge present in the left or right bath, using the following equation:

$I_g(t) = \frac{d \int f(x, t) Q(x) dx}{dt}$ where $I_g(t)$ represents the time-dependent gating current, $Q(x)$ the net charge found in the left (or right)

¹¹ We wish to stress that due to the stochastic nature of the voltage sensor, even a full understanding of its dynamics—that we think our model is able to provide—does not allow to predict the dynamics of a population of voltage sensors, i.e., the macroscopic gating currents.

bath, and the integration goes for all possible positions of the voltage sensor.

The trace reported in Fig. 5a shows a simulated macroscopic gating current obtained in response to a membrane depolarization from -80 to -20 mV using the method illustrated above. Notice that this current has been obtained using a probability density function whose overall integral is unity; thus, it represents the current contributed by the movement of only one voltage sensor. This current should therefore be multiplied by the number of voltage sensors present in the membrane under study to obtain the real macroscopic gating current. Several features of the simulated response recall those observed in biophysical experiments (cf. Fig. 1b). First, in the few tens of microseconds from the beginning of the depolarizing step, a very fast gating current component appears, rising instantaneously and falling very rapidly. Second, this fast component is followed by a second slower component starting with a rising phase and continuing with a slow decay (Fig. 5a, d). Both these features have been observed experimentally, using high-speed recordings [8, 77].

To understand the origin of the fast gating current component, we looked at the probability density function of the voltage sensor position before the depolarizing step, and 100 μ s after the beginning of the depolarization. During this short time, the voltage sensor does not have the chance to change its sub-state. There is however a slight redistribution of the voltage sensors within the energy well of state 1 (Fig. 5b), and this is what we think gives rise to the fast gating current component. This slight redistribution originates from a change in the energetic landscape due to the change in applied voltage (Fig. 5b, upper plot).

We then focused on the mechanism that could explain the properties of the slower component of the gating current, i.e., the plateau/rising phase followed by the decaying phase. From the analysis of some critical variable of the model (not shown), it appears that this behavior could be due to the initial coherent outward movement of S4s that share a similar position at the beginning of the depolarization. This consonant movement would bring the first gating charge of virtually all S4s to enter coherently the gating pore within few hundreds microseconds from the beginning of the depolarization (Fig. 5c). Since most of the voltage drop occurs inside this high resistance region, the force acting on S4s increases substantially during this interval, leading to a marked increase in the particle velocity and gating current. Looking at this process from another point of view, and taking into account the Fokker-Planck Eq. (3), we may think of the movement of S4s as made up of a voltage driven (drift) term $-\frac{1}{\gamma} \times \frac{\partial(F_{ex}(t)f(x, t))}{\partial x}$ and a diffusive term $\frac{k_B T}{\gamma} \frac{\partial^2 f(x, t)}{\partial x^2}$. If the drift term is sufficiently high as compared with the diffusive

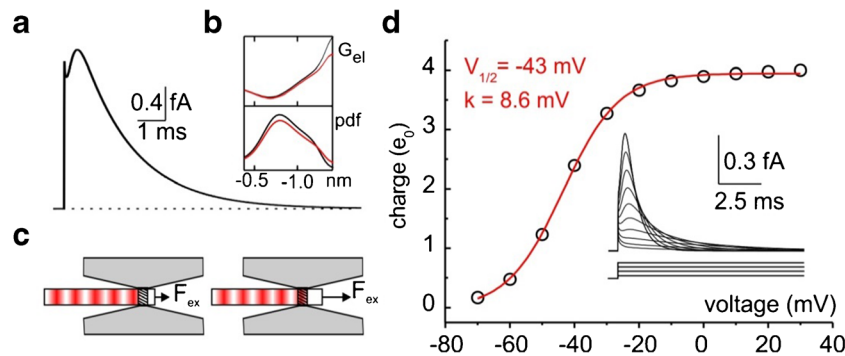


Fig. 5 **a** Simulated macroscopic gating current evoked by a voltage pulse from -80 to -20 mV, using the model described in the text. **b** Energy profiles, G_{el} , of the deactivated state (the most leftward in Fig. 4b, bottom) and corresponding probability density functions, pdf, of the S4 segment at -80 mV (black), and $100 \mu\text{s}$ from the beginning of the depolarizing step

(red) for the simulation shown in panel **a**. **c** Drawings showing that upon depolarization the R1 charges enter coherently the gating pore, causing an increase in the force acting on the voltage sensor. **d** Plot of the gating charge, obtained as the integral of the simulated macroscopic gating currents shown in inset, as a function of the applied voltage

term (i.e., at relatively depolarized voltages), then S4s will all move outwards at a very similar speed, and this will determine the oscillating behavior of the force and of the gating current.

In conclusion, the simulations reported above demonstrate that the Brownian formalism is capable to predict the main features of the gating currents recorded from Kv channels, and give a physical explanation to the observed properties. A more detailed comparison with experimental data from *Shaker* Kv channels may be found in our recent paper [13].

Shortcomings of Brownian modeling approach

We have shown that the description of S4 as a Brownian particle allows to follow its trajectory for times long enough to fully cover the voltage-dependent activation (gating) process. This marks a significant improvement when compared with MD, where observation times in the multimillisecond domain is still prohibitive. With Brownian dynamics, also the behavior of a population of channels may easily be assessed and used to predict the macroscopic gating current. Brownian dynamics applied to channel's voltage gating has, however, its shortcomings. The most obvious, and shared by all reduced physical models, is the presence of free parameters whose exact quantitative values are unknown, yet they need be included in the model in order to account for the effects of what has not been explicitly considered. On the other hand, the presence of these free parameters may significantly reduce the predicting power of the model, since they are adjusted to make the model fit the experimental data. In the reduced Brownian model shown here, we have at least two such free parameters: the frictional coefficient γ appearing in the stochastic differential equation and Fokker-Planck equation, describing the frictional effect that water and surrounding protein structures have on S4, and the relative dielectric constant ϵ , which accounts for the effect of these same structures on the electrostatic forces acting on the gating charges.

To overcome this problem, we are presently working at a multiscale modeling approach, often applied in quantitative sciences, where a series of hierarchical computational methods are linked in a way that the calculated quantities from a computational simulation at a lower scale are used to define the parameters of the model at a larger scale. In the case of voltage-dependent gating, the idea translates into determining the free parameters present in the Brownian model of voltage gating by using MD simulations performed on the available crystal structures of the voltage sensor domain. This approach appears feasible since the assessment of the free parameters is usually much less computationally demanding than building up a full model.

Conclusions and outlook

In this review we have presented the basic available data useful to understand the voltage-dependent gating in Kv channels, and described a new modeling approach to investigate the voltage-dependent gating mechanism of ion channels that treats the charged S4 segment of the voltage sensor domain as a Brownian particle subjected to electro-diffusion. One of the major gains of this approach is that it allows to alternatively describe the dynamics of a single S4 segment, using the Langevin's stochastic differential equation, or the behavior of a population of S4 segments, useful to assess the macroscopic gating current, using the Fokker-Planck equation. We also showed that the Brownian model qualitatively predicts all the main features of the *Shaker* channel voltage-dependent gating, and explains them in terms of the electrostatic potential profile originating from all the charges present in the system. Namely, it reproduces the stable intermediate states of S4, corresponding to the various positions S4 can take, that had initially been suggested by studying the gating currents with Markovian approaches, and more recently confirmed by MD simulations. The model also predicts the fast component of the

macroscopic gating current, at the beginning of a depolarizing and repolarizing step, and suggests that it originates from a redistribution of the S4 population within the two most extreme energy wells (fully activated and fully deactivated) following a step change in the applied voltage. Another property of the voltage sensor dynamics well reproduced by the Brownian model is the peculiar time course of the macroscopic gating current for relatively high depolarizing steps, consisting of a rising phase followed by a slower decay.

The simplified model presented here cannot account for other features of the gating mechanism, since provisions for them have not been included. First, since it has been developed in one dimension, the model is not capable to account for rotational effects of S4 while it moves along the activation pathway. This counterclockwise rotation of S4 by about 180° allows to position the gating charges at all times close to the countercharges present on the other segments of the VSD, thus maximizing their electrostatic interaction. Second, other types of interactions such as van der Waals, and π -cation have not been included here, yet they may significantly contribute to the stability of the various kinetic states of the VSD. Finally, the model considers only one of the four VSDs contributing to the gating of an ion channel, and thus it cannot be used to explore cooperative interactions between the different channel subunits, which experimental results suggest to occur and be relevant to the gating process. Notably, the failure of the model to predict a double Boltzmann, as found in experimental Q-V relationships, is almost certainly due to the lack of a cooperative, inter-subunit conformational change.

Provisions to account for these aspects of the gating mechanism not met by the present model may however be fairly easily introduced. Future developments of a 3D Brownian model at which we are presently working will better describe the conformational changes of S4 during voltage-dependent gating. Second, the contribution of non-electrostatic interactions could easily be introduced in the Langevin and Fokker-Planck equations in the form of an additional external force contributing to the drift term. Third, the model may be easily expanded to include four interacting VSDs controlling a single channel gate, which would furthermore confer the possibility to predict ion currents in addition to gating currents, thus increasing the available experimental data that can be used to understand the physics of the voltage-dependent gating in ion channels.

Finally, we wish to mention a recent work from Catterall's group who has provided the first 3D structure of a Nav channel in the resting conformation [94]. This is an extremely important observation as it has allowed for the first time to directly compare the resting and the activated conformation of the channel. The results from this comparison support a classical sliding helix mechanism of voltage gating, with the S4 segment passing three gating charges from the

extracellular to the intracellular vestibule during closing (and opening). They also show the formation of an intracellularly directed "elbow" made of the intracellular part of S4 and the S4–S5 linker, which results in a constriction of the S4–S5 linkers towards the S6 transmembrane segments, and in the pore closing. It would be interesting to build a Brownian model of Nav channel gating incorporating this structural information on the closed and open state, not presently available for *Shaker*, and see whether the macroscopic gating currents originating from these channels and the number of gating charges passing the gating pore are correctly reproduced. The resulting model could be very useful to understand the physical forces that drive the voltage gating of Nav channels.

Acknowledgements This work was supported by Progetto Ricerca di Base 2017, Department of Chemistry, Biology and Biotechnology, University of Perugia and by Progetto Ricerca Finalizzata 2018 #RF-2018-12366215.

Authors' contribution LC developed the Brownian model of channel gating; LC and FF designed and wrote the first draft of the Ms; LC, LS, and FF discussed and amended the first draft, and finalized the Ms.

References

1. Aggarwal SK, MacKinnon R (1996) Contribution of the S4 segment to gating charge in the Shaker K⁺ channel. *Neuron* 16:1169–1177
2. Ahern CA, Horn R (2005) Focused electric field across the voltage sensor of potassium channels. *Neuron* 48:25–29
3. Alberts IL, Nadassy K, Wodak SJ (1998) Analysis of zinc binding sites in protein crystal structures. *Protein Sci* 7:1700–1716
4. Armstrong CM (1981) Sodium channels and gating currents. *Physiol Rev* 61:644–683
5. Armstrong CM, Bezanilla F (1973) Currents related to movement of the gating particles of the sodium channels. *Nature* 242(5398):459–461
6. Asamoah OK, Wuskell JP, Loew LM, Bezanilla F (2003) A fluorometric approach to local electric field measurements in a voltage-gated ion channel. *Neuron* 37:85–97
7. Batulan Z, Haddad GA, Blunck R (2010) An intersubunit interaction between S4-S5 linker and S6 is responsible for the slow off-gating component in Shaker K⁺ channels. *J Biol Chem* 285:14005–14019. <https://doi.org/10.1074/jbc.M109.097717>
8. Bezanilla F (2000) The voltage sensor in voltage-dependent ion channels. *Physiol Rev* 80:555–592
9. Bezanilla F, Perozo E, Papazian DM, Stefani E (1991) Molecular basis of gating charge immobilization in Shaker potassium channels. *Science* 254(5032):679–683
10. Bezanilla F, Perozo E, Stefani E (1994) Gating of Shaker K⁺ channels: II. The components of gating currents and a model of channel activation. *Biophys J* 66:1011–1021
11. Blunck R, Batulan Z (2012) Mechanism of electromechanical coupling in voltage-gated potassium channels. *Front Pharmacol* 3:166. <https://doi.org/10.3389/fphar.2012.00166>
12. Campos FV, Chanda B, Roux B, Bezanilla F (2007) Two atomic constraints unambiguously position the S4 segment relative to S1 and S2 segments in the closed state of Shaker K channel. *Proc Natl Acad Sci U S A* 104:7904–7909

13. Catacuzzeno L, Franciolini F (2019) Simulation of gating currents of the Shaker K channel using a Brownian model of the voltage sensor. *Biophys J* 117(10):2005–2019
14. Catacuzzeno L, Fioretti B, Franciolini F (2008) Modeling study of the effects of membrane surface charge on calcium microdomains and neurotransmitter release. *Biophys J* 95(5):2160–2171
15. Catterall WA (1986) Molecular properties of voltage-sensitive sodium channels. *Annu Rev Biochem* 55:953–985
16. Catterall WA (1988) Structure and function of voltage-sensitive ion channels. *Science* 242(4875):50–61
17. Cha A, Snyder GE, Selvin PR, Bezanilla F (1999) Atomic scale movement of the voltage-sensing region in a potassium channel measured via spectroscopy. *Nature* 402(6763):809–813
18. Chanda B, Asamoah OK, Blunck R, Roux B, Bezanilla F (2005) Gating charge displacement in voltage-gated ion channels involves limited trans membrane movement. *Nature* 436(7052):852–856
19. Chupin L (2010) Fokker-Planck equation in bounded domain. *Annales de l'Institut Fourier* 60:217–255
20. Conti F, Stühmer W (1989) Quantal charge redistributions accompanying the structural transitions of sodium channels. *Eur Biophys J* 17(2):53–59
21. Cooper K, Jakobsson E, Wolyne P (1985) The theory of ion transport through membrane channels. *Prog Biophys Mol Biol* 46(1): 51–96
22. DeCaen PG, Yarov-Yarovoy V, Zhao Y, Scheuer T, Catterall WA (2008) Disulfide docking a sodium channel voltage sensor reveals ion pair formation during activation. *Proc Natl Acad Sci U S A* 105: 15142–15147. <https://doi.org/10.1073/pnas.0806486105>
23. DeCaen PG, Yarov-Yarovoy V, Sharp EM, Scheuer T, Catterall WA (2009) Sequential formation of ion pairs during activation of a sodium channel voltage sensor. *Proc Natl Acad Sci U S A* 106: 22498–22503. <https://doi.org/10.1073/pnas.0912307106>
24. DeCaen PG, Yarov-Yarovoy V, Scheuer T, Catterall WA (2011) Gating charge interactions with the S1 segment during activation of a Na⁺ channel voltage sensor. *Proc Natl Acad Sci U S A* 108: 18825–18830. <https://doi.org/10.1073/pnas.1116449108>
25. Delemotte L, Treptow W, Klein ML, Tarek M (2010) Effect of sensor domain mutations on the properties of voltage-gated ion channels: molecular dynamics studies of the potassium channel Kv1.2. *Biophys J* 99:L72–L74. <https://doi.org/10.1016/j.bpj.2010.08.069>
26. Delemotte L, Tarek M, Klein ML, Amaral C, Treptow W (2011) Intermediate states of the Kv1.2 voltage sensor from atomistic molecular dynamics simulations. *Proc Natl Acad Sci U S A* 108:6109–6114. <https://doi.org/10.1073/pnas.1102724108>
27. Dryga A, Chakrabarty S, Vicatos S, Warshel A (2012a) Realistic simulation of the activation of voltage-gated ion channels. *Proc Natl Acad Sci U S A* 109:3335–3340. <https://doi.org/10.1073/pnas.1121094109>
28. Dryga A, Chakrabarty S, Vicatos S, Warshel A (2012b) Coarse grained model for exploring voltage dependent ion channels. *Biochim Biophys Acta* 1818:303–317. <https://doi.org/10.1016/j.bbamem.2011.07.043>
29. Gandhi CS, Clark E, Loots E, Pralle A, Isacoff EY (2003) The orientation and molecular movement of a K(+) channel voltage-sensing domain. *Neuron* 40:515–525
30. Glauner KS, Mannuzzu LM, Gandhi CS, Isacoff EY (1999) Spectroscopic mapping of voltage sensor movement in the Shaker potassium channel. *Nature* 402(6763):813–817
31. Greenblatt RE, Blatt Y, Montal M (1985) The structure of the voltage-sensitive sodium channel. Inferences derived from computer-aided analysis of the Electrophorus electricus channel primary structure. *FEBS Lett* 193:125–134
32. Guy HR, Seetharamulu P (1986) Molecular model of the action potential sodium channel. *Proc Natl Acad Sci U S A* 83(2):508–512
33. Haddad GA, Blunck R (2011) Mode shift of the voltage sensors in Shaker K⁺ channels is caused by energetic coupling to the pore domain. *J Gen Physiol* 137(5):455–472. <https://doi.org/10.1085/jgp.201010573>
34. Henrion U, Renhorn J, Börjesson SI, Nelson EM, Schwaiger CS, Bjelkmar P, Wallner B, Lindahl E, Elinder F (2012) Tracking a complete voltage-sensor cycle with metal-ion bridges. *Proc Natl Acad Sci U S A* 109:8552–8557. <https://doi.org/10.1073/pnas.1116938109>
35. Hodgkin AL, Huxley AF (1952) A quantitative description of membrane current and its application to conduction and excitation in nerve. *J Physiol* 117:500–544
36. Horng TL, Eisenberg RS, Liu C, Bezanilla F (2019) Continuum gating current models computed with consistent interactions. *Biophys J* 116:270–282. <https://doi.org/10.1016/j.bpj.2018.11.3140>
37. Islas LD, Sigworth FJ (2001) Electrostatics and the gating pore of Shaker potassium channels. *J Gen Physiol* 117:69–89
38. Jensen MØ, Jogini V, Borhani DW, Leffler AE, Dror RO, Shaw DE (2012) Mechanism of voltage gating in potassium channels. *Science* 336(6078):229–233. <https://doi.org/10.1126/science.1216533>
39. Jiang Y, Lee A, Chen J, Ruta V, Cadene M, Chait BT, MacKinnon R (2003) X-ray structure of a voltage-dependent K⁺ channel. *Nature* 423(6935):33–41
40. Kalstrup T, Blunck R (2013) Dynamics of internal pore opening in K(V) channels probed by a fluorescent unnatural amino acid. *Proc Natl Acad Sci U S A* 110:8272–8277. <https://doi.org/10.1073/pnas.1220398110>
41. Kalstrup T, Blunck R (2018) S4-S5 linker movement during activation and inactivation in voltage-gated K(+) channels. *Proc Natl Acad Sci U S A* 115:E6751–E6759. <https://doi.org/10.1073/pnas.1719105115>
42. Keynes RD, Rojas E (1974) Kinetics and steady-state properties of the charged system controlling sodium conductance in the squid giant axon. *J Physiol* 239:393–434
43. Khalili-Araghi F, Jogini V, Yarov-Yarovoy V, Tajkhorshid E, Roux B, Schulten K (2010) Calculation of the gating charge for the Kv1.2 voltage-activated potassium channel. *Biophys J* 98:2189–2198. <https://doi.org/10.1016/j.bpj.2010.02.056>
44. Kim I, Warshel A (2014) Coarse-grained simulations of the gating current in the voltage-activated Kv1.2 channel. *Proc Natl Acad Sci U S A* 111:2128–2133. <https://doi.org/10.1073/pnas.1324014111>
45. Labro AJ, Raes AL, Grottesi A, Van Hoorick D, Sansom MS, Snyders DJ (2008) Kv channel gating requires a compatible S4-S5 linker and bottom part of S6, constrained by non-interacting residues. *J Gen Physiol* 132:667–680. <https://doi.org/10.1085/jgp.200810048>
46. Lacroix JJ, Campos FV, Frezza L, Bezanilla F (2013) Molecular bases for the asynchronous activation of sodium and potassium channels required for nerve impulse generation. *Neuron* 79(4): 651–657. <https://doi.org/10.1016/j.neuron.2013.05.036>
47. Lacroix JJ, Hyde HC, Campos FV, Bezanilla F (2014) Moving gating charges through the gating pore in a Kv channel voltage sensor. *Proc Natl Acad Sci U S A* 111:E1950–E1959. <https://doi.org/10.1073/pnas.1406161111>
48. Larsson HP, Baker OS, Dhillon DS, Isacoff EY (1996) Transmembrane movement of the Shaker K⁺ channel S4. *Neuron* 16:387–397
49. Lemons DS, Gythiel A (1997) Paul Langevin's 1908 paper "On the Theory of Brownian Motion" ["Sur la théorie du mouvement brownien," *C. R. Acad. Sci. (Paris)* 146, 530–533 (1908)]. *Am J Phys* 65:1079–1081. <https://doi.org/10.1119/1.18725>
50. Lin MC, Hsieh JY, Mock AF, Papazian DM (2011) R1 in the Shaker S4 occupies the gating charge transfer center in the resting

- state. *J Gen Physiol* 138:155–163. <https://doi.org/10.1085/jgp.201110642>
51. Li-Smerin Y, Hackos DH, Swartz KJ (2000) A localized interaction surface for voltage-sensing domains on the pore domain of a K⁺ channel. *Neuron* 25:411–423
 52. Long SB, Campbell EB, Mackinnon R (2005) Crystal structure of a mammalian voltage-dependent Shaker family K⁺ channel. *Science* 309(5736):897–903
 53. Long SB, Tao X, Campbell EB, MacKinnon R (2007) Atomic structure of a voltage-dependent K⁺ channel in a lipid membrane-like environment. *Nature* 450(7168):376–382
 54. Lu Z, Klem AM, Ramu Y (2001) Ion conduction pore is conserved among potassium channels. *Nature* 413(6858):809–813
 55. Lu Z, Klem AM, Ramu Y (2002) Coupling between voltage sensors and activation gate in voltage-gated K⁺ channels. *J Gen Physiol* 120:663–676
 56. Ma LJ, Ohmert I, Vardanyan V (2011) Allosteric features of KCNQ1 gating revealed by alanine scanning mutagenesis. *Biophys J* 100(4):885–894. <https://doi.org/10.1016/j.bpj.2010.12.3726>
 57. McCammon JA, Gelin BR, Karplus M (1977) Dynamics of folded proteins. *Nature*. 267(5612):585–590
 58. McCormack K, Joiner WJ, Heinemann SH (1994) A characterization of the activating structural rearrangements in voltage-dependent Shaker K⁺ channels. *Neuron* 12:301–315
 59. Noceti F, Baldelli P, Wei X, Qin N, Toro L, Birnbaumer L, Stefani E (1996) Effective gating charges per channel in voltage-dependent K⁺ and Ca²⁺ channels. *J Gen Physiol* 108:143–155
 60. Noda M, Shimizu S, Tanabe T, Takai T, Kayano T, Ikeda T, Takahashi H, Nakayama H, Kanaoka Y, Minamino N et al (1984) Primary structure of *Electrophorus electricus* sodium channel deduced from cDNA sequence. *Nature* 312(5990):121–127
 61. Papazian DM, Schwarz TL, Tempel BL, Jan YN, Jan LY (1987) Cloning of genomic and complementary DNA from Shaker, a putative potassium channel gene from *Drosophila*. *Science* 237(4816):749–753
 62. Papazian DM, Shao XM, Seoh SA, Mock AF, Huang Y, Wainstock DH (1995) Electrostatic interactions of S4 voltage sensor in Shaker K⁺ channel. *Neuron* 14:1293–1301
 63. Pathak MM, Yarov-Yarovoy V, Agarwal G, Roux B, Barth P, Kohout S, Tombola F, Isacoff EY (2007) Closing in on the resting state of the Shaker K(+) channel. *Neuron* 56:124–140
 64. Peyser A, Nonner W (2012a) Voltage sensing in ion channels: mesoscale simulations of biological devices. *Phys Rev E Stat Nonlin Soft Matter Phys* 86:011910
 65. Peyser A, Nonner W (2012b) The sliding-helix voltage sensor: mesoscale views of a robust structure-function relationship. *Eur Biophys J* 41:705–721. <https://doi.org/10.1007/s00249-012-0847-z>
 66. Pongs O, Kecskemethy N, Müller R, Krah-Jentgens I, Baumann A, Kiltz HH, Canal I, Llamazares S, Ferrus A (1988) Shaker encodes a family of putative potassium channel proteins in the nervous system of *Drosophila*. *EMBO J* 7(4):1087–1096
 67. Posson DJ, Selvin PR (2008) Extent of voltage sensor movement during gating of Shaker K⁺ channels. *Neuron* 59:98–109. <https://doi.org/10.1016/j.neuron.2008.05.006>
 68. Posson DJ, Ge P, Miller C, Bezanilla F, Selvin PR (2005) Small vertical movement of a K⁺ channel voltage sensor measured with luminescence energy transfer. *Nature* 436(7052):848–851
 69. Pusch M, Noda M, Stühmer W, Numa S, Conti F (1991) Single point mutations of the sodium channel drastically reduce the pore permeability without preventing its gating. *Eur Biophys J* 20:127–133
 70. Schneider MF, Chandler WK (1973) Voltage dependent charge movement of skeletal muscle: a possible step in excitation-contraction coupling. *Nature* 242(5395):244–246
 71. Schoppa NE, Sigworth FJ (1998) Activation of Shaker potassium channels: I. Characterization of voltage-dependent transitions. *J Gen Physiol* 111:271–294
 72. Schoppa NE, McCormack K, Tanouye MA, Sigworth FJ (1992) The size of gating charge in wild-type and mutant Shaker potassium channels. *Science* 255(5052):1712–1715
 73. Schwaiger CS, Bjelkmar P, Hess B, Lindahl E (2011) ₃₁₀-helix conformation facilitates the transition of a voltage sensor S4 segment toward the down state. *Biophys J* 100:1446–1454. <https://doi.org/10.1016/j.bpj.2011.02.003>
 74. Seoh SA, Sigg D, Papazian DM, Bezanilla F (1996) Voltage-sensing residues in the S2 and S4 segments of the Shaker K⁺ channel. *Neuron* 16:1159–1167
 75. Shrivastava IH, Durell SR, Guy HR (2004) A model of voltage gating developed using the KvAP channel crystal structure. *Biophys J* 87(4):2255–2270
 76. Sigg D, Stefani E, Bezanilla F (1994) Gating current noise produced by elementary transitions in Shaker potassium channels. *Science* 264(5158):578–582
 77. Sigg D, Bezanilla F, Stefani E (2003) Fast gating in the Shaker K⁺ channel and the energy landscape of activation. *Proc Natl Acad Sci U S A* 100:7611–7615
 78. Smith-Maxwell CJ, Ledwell JL, Aldrich RW (1998) Uncharged S4 residues and cooperativity in voltage-dependent potassium channel activation. *J Gen Physiol* 111:421–439
 79. Soler-Llavina GJ, Chang TH, Swartz KJ (2006) Functional interactions at the interface between voltage-sensing and pore domains in the Shaker K(v) channel. *Neuron* 52:623–634
 80. Starace DM, Bezanilla F (2001) Histidine scanning mutagenesis of basic residues of the S4 segment of the Shaker K⁺ channel. *J Gen Physiol* 117:469–490
 81. Starace DM, Bezanilla F (2004) A proton pore in a potassium channel voltage sensor reveals a focused electric field. *Nature* 427(6974):548–553
 82. Starace DM, Stefani E, Bezanilla F (1997) Voltage-dependent proton transport by the voltage sensor of the Shaker K⁺ channel. *Neuron* 19:1319–1327
 83. Stühmer W, Conti F, Suzuki H, Wang XD, Noda M, Yahagi N, Kubo H, Numa S (1989) Structural parts involved in activation and inactivation of the sodium channel. *Nature* 339(6226):597–603
 84. Stühmer W, Conti F, Stocker M, Pongs O, Heinemann SH (1991) Gating currents of inactivating and non-inactivating potassium channels expressed in *Xenopus* oocytes. *Pflugers Arch* 418:423–429
 85. Tao X, Lee A, Limapichat W, Dougherty DA, MacKinnon R (2010) A gating charge transfer center in voltage sensors. *Science* 328(5974):67–73. <https://doi.org/10.1126/science.1185954>
 86. Tiwari-Woodruff SK, Schulteis CT, Mock AF, Papazian DM (1997) Electrostatic interactions between transmembrane segments mediate folding of Shaker K⁺ channel subunits. *Biophys J* 72(4):1489–1500
 87. Tiwari-Woodruff SK, Lin MA, Schulteis CT, Papazian DM (2000) Voltage-dependent structural interactions in the Shaker K(+) channel. *J Gen Physiol* 115(2):123–138
 88. Tombola F, Pathak MM, Isacoff EY (2005) Voltage-sensing arginines in a potassium channel permeate and occlude cation-selective pores. *Neuron* 45(3):379–388
 89. Tombola F, Pathak MM, Gorostiza P, Isacoff EY (2007) The twisted ion-permeation pathway of a resting voltage-sensing domain. *Nature* 445(7127):546–549
 90. Tytgat J, Hess P (1992) Evidence for cooperative interactions in potassium channel gating. *Nature* 359(6394):420–423
 91. Vardanyan V, Pongs O (2012) Coupling of voltage-sensors to the channel pore: a comparative view. *Front Pharmacol* 3:145. <https://doi.org/10.3389/fphar.2012.00145>

92. Vargas E, Bezanilla F, Roux B (2011) In search of a consensus model of the resting state of a voltage-sensing domain. *Neuron* 72(5):713–720. <https://doi.org/10.1016/j.neuron.2011.09.024>
93. Vargas E, Yarov-Yarovoy V, Khalili-Araghi F, Catterall WA, Klein ML, Tarek M, Lindahl E, Schulten K, Perozo E, Bezanilla F, Roux B (2012) An emerging consensus on voltage-dependent gating from computational modeling and molecular dynamics simulations. *J Gen Physiol* 140:587–594. <https://doi.org/10.1085/jgp.201210873>
94. Wisedchaisri G, Tonggu L, McCord E, Gamal El-Din TM, Wang L, Zheng N, Catterall WA (2019) Resting-state structure and gating mechanism of a voltage-gated sodium channel. *Cell* 178:993–1003
95. Yang N, George AL Jr, Horn R (1996) Molecular basis of charge movement in voltage-gated sodium channels. *Neuron*. 16(1):113–122
96. Yarov-Yarovoy V, Baker D, Catterall WA (2006) Voltage sensor conformations in the open and closed states in ROSETTA structural models of K(+) channels. *Proc Natl Acad Sci U S A* 103:7292–7297
97. Yarov-Yarovoy V, DeCaen PG, Westenbroek RE, Pan CY, Scheuer T, Baker D, Catterall WA (2012) Structural basis for gating charge movement in the voltage sensor of a sodium channel. *Proc Natl Acad Sci U S A* 109:E93–E102. <https://doi.org/10.1073/pnas.1118434109>
98. Zagotta WN, Hoshi T, Aldrich RW (1994) Shaker potassium channel gating. III: Evaluation of kinetic models for activation. *J Gen Physiol* 103:321–362

Publisher's note Springer Nature remains neutral with regard to jurisdictional claims in published maps and institutional affiliations.